Journal of Mathematical Chemistry Vol. 30, No. 2, August 2001 (© 2001)

Stochastic and deterministic simulation of nonisothermal crystallization of polymers

Alessandra Micheletti [a] and Martin Burger [b]

[a] *MIRIAM and Dipartimento di Matematica, Università degli Studi di Milano, Via Saldini 50, 20133 Milano, Italy*
E-mail: Alessandra.Micheletti@mat.unimi.it

[b] *Industrial Mathematics Institute, Johannes Kepler Universität Linz, Altenbergerstr. 69, 4040 Linz, Austria*
E-mail: burger@indmath.uni-linz.ac.at

Received 14 September 2000; revised 18 October 2001

This paper is devoted to the numerical simulation of nonisothermal crystallization of polymers, which may be modelled as a stochastic birth-and-growth process. One of the main aims is to develop efficient algorithms for the stochastic simulation of such process. We put a special emphasis on the problem of computing the surface density of crystals, which is an important factor for the mechanical properties of the solidified material. Moreover, an averaged deterministic model, designed as an approximation in the case of many small crystals (which is very frequent in industrial applications), is presented, and the results of numerical simulations are compared with the corresponding simulations of the stochastic model.

KEY WORDS: polymer crystallization, stochastic simulation, random differential equations, mathematical morphology

1. Introduction

This paper is devoted to the numerical simulation of nonisothermal crystallization of polymers, which is a topic of growing interest in material science and chemistry with many relevant industrial applications. A crystallization process is in general the superposition of two basic features, namely *nucleation* and *growth* of crystals. While the growth process may be considered deterministic (with normal speed $G = G(x, t)$, the *growth rate*, depending upon the temperature field), nucleation occurs randomly in space and time (the kinetic parameters being themselves temperature dependent). We will consider a crystallization process in a bounded domain $E \subset \mathbb{R}^d$ ($d = 1, 2, 3$) and assume that nucleation takes place only in the interior of E.

We will denote by Θ^t the crystalline phase at time t and by $\Theta^t(X_0, T_0)$ a crystal born at point X_0 at time T_0 and freely grown up to time t. In a crystallization process with nucleation events $\{(X_j, T_j) \mid 0 \leqslant T_1 \leqslant T_2 \leqslant \cdots\}$, the crystalline phase at time t is given by

0259-9791/01/0800-0169$19.50/0

$$\Theta^t = \bigcup_{T_j < t} \Theta^t(X_j, T_j). \tag{1.1}$$

Note that because of the stochasticity of nucleation, the set Θ^t is stochastic and since in a bounded space-time region it is also closed and bounded, hence, it is a *random compact set* (RACS) [1]. It turns out (cf. [2,3]) that on a macroscopic scale the quantity

$$\xi(x,t) := E\big[I_{\Theta^t}(x)\big] = P\big(\{x \in \Theta^t\}\big), \quad x \in E,\ t \in \mathbb{R}_+ \tag{1.2}$$

(usually called *crystallinity* or *local volume density*) is suitable for the description of the crystallization process in many cases relevant in practice. In the simple case of spatially homogenous growth and nucleation, equations for ξ (which is then a function of time only) can be derived based upon the classical approaches by Avrami, Kolmogorov and Evans (cf. [4–6]). These models yield a good description of isothermal processes and have been investigated frequently in bounded and unbounded domains (cf. [3,7–10]).

In many applications further characteristics of the final morphology are of interest, in particular the interfaces between the crystals (see figure 1), which heavily influence the mechanical properties of the material (cf. [11]). Because of impingement, at a certain time t of the crystallization process the available space is randomly divided into cells, forming a so called (*incomplete*) *Johnson–Mehl tessellation* [12,13] (the tessellation is incomplete at time t if some uncrystallized space is still available). In the following $\tau_i(y)$ will denote the time at which a point $y \in E$ is reached by the crystal freely grown (disregarding impingement) from the nucleus $a_i = (X_i, T_i)$. If the point is never covered by the ith crystal, we formally write $\tau_i(y) = \infty$.

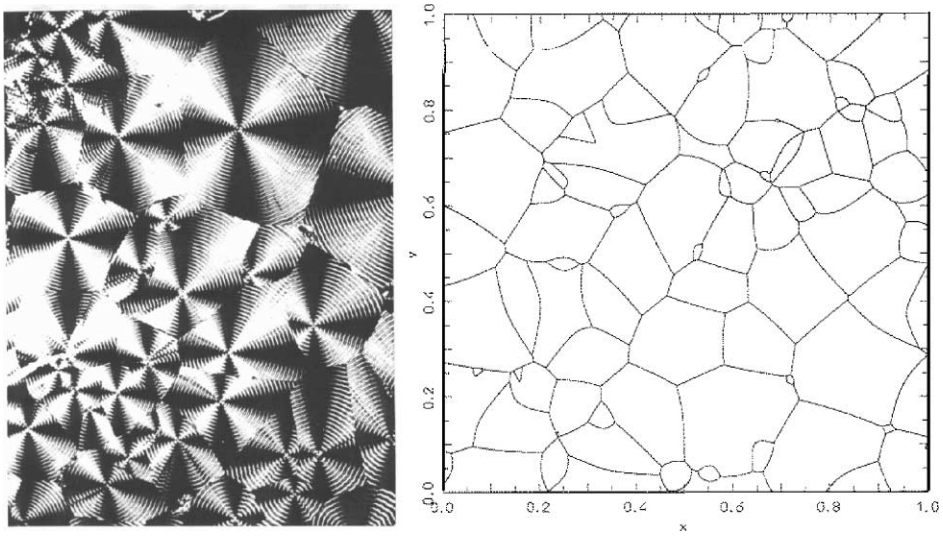

Figure 1. The Johnson–Mehl tessellation generated in a polymer crystallization process in experiment (left) and numerical simulation (right).

Definition 1.1. The *crystal* $C_i(t)$ of the (incomplete) tessellation, generated by the nucleus $a_i = (X_i, T_i)$, at the time of observation t is the non-empty set

$$C_i(t) = \{y \in E \mid \tau_i(y) \leqslant t \text{ and } \tau_i(y) \leqslant \tau_j(y)\ \forall j \neq i\}.$$

We will denote by $C_e(t)$ the uncrystallized region at time t, i.e.,

$$C_e(t) := \{y \in E \mid \tau_i(y) > t,\ \forall i \in \mathbb{N}\}.$$

In order to describe rigorously the concept of "interface" between crystals, we introduce the definition of *n-facet* (cf. also [12–14]):

Definition 1.2. An *n-facet* ($0 \leqslant n \leqslant d$) is the non-empty intersection between $m+1$ crystals or between m crystals and the amorphous region, i.e.,

$$F_n(t, a_{k_0}, \ldots, a_{k_m}) = C_{k_0}(t) \cap C_{k_1}(t) \cap \cdots \cap C_{k_m}(t),$$

with $m = d - n$ and $k_0, \ldots, k_m \in \mathbb{N} \cup \{e\}$.

Note that in the previous definitions d denotes the dimension of the space in which the tessellation takes place, n denotes the dimension of the interface under consideration, and $m+1$ denotes the number of crystals involved in the formation of such an interface, if we consider the amorphous region as a particular crystal itself. E.g., in the case $d = 2$, a 2-facet is a crystal, a 1-facet is the boundary of a crystal and a 0-facet is a vertex of a crystal (see figure 2). Note also that F_n is a stochastic quantity, depending on the random space-time point process $\{a_k\}_{k\in\mathbb{N}}$.

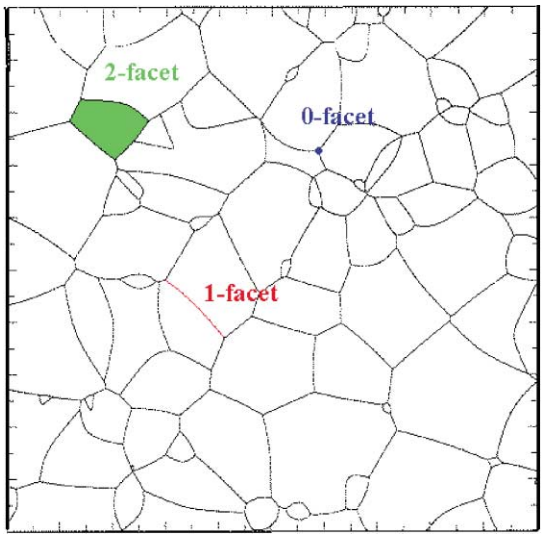

Figure 2. Examples of an incomplete Johnson–Mehl tessellation and n-facets in two spatial dimensions.

For a Borel set B one can define the *stochastic* and the *mean* content of n-facets at time t in B:

Definition 1.3. We call *stochastic content of n-facets* at time t in the Borel set $B \subset E$ the quantity

$$\widetilde{\mathcal{M}}_{d,n}(t, B) = \frac{1}{(m+1)!}\left[\sum_{a_{k_0},\dots,a_{k_m}}^{\neq} \lambda_n\big(B \cap F_n(t, a_{k_0}, \dots, a_{k_m})\big)\right], \tag{1.3}$$

where λ_n is the n-dimensional Hausdorff measure and the symbol $\neq$ denotes that the nuclei $a_{k_0}, \dots, a_{k_m}$ must be distinct.

Definition 1.4. We call *mean content of n-facets* at time t in the Borel set $B \subset E$ the quantity

$$\begin{aligned}\mathcal{M}_{d,n}(t, B) &= E\big(\widetilde{\mathcal{M}}_{d,n}(t, B)\big) \\ &= \frac{1}{(m+1)!} E\left[\sum_{a_{k_0},\dots,a_{k_m}}^{\neq} \lambda_n\big(B \cap F_n(t, a_{k_0}, \dots, a_{k_m})\big)\right].\end{aligned} \tag{1.4}$$

If the measure $\mathcal{M}_{d,n}(t, \cdot)$ is absolutely continuous with respect to the d-dimensional Lebesgue measure ν_d, then there exists a density (i.e., the Radon–Nikodym derivative of $\mathcal{M}_{d,n}$ with respect to ν_d) $\mu_{d,n}(t, x)$ such that for all Borel sets B in E

$$\mathcal{M}_{d,n}(t, B) = \int_B \mu_{d,n}(t, x)\, \mathrm{d}x. \tag{1.5}$$

Definition 1.5. The function $\mu_{d,n}(t, x)$ defined by (1.5) is called *local mean density of n-facets* of the (incomplete) tessellation at time t.

If the birth-and-growth process that generates the tessellation is spatially homogeneous (which means in our case that the temperature field is constant in space), the density $\mu_{d,n}(t, x)$ does not depend on the spatial location x (cf. [14] for a detailed discussion of this case).

In the following we discuss problems related to the numerical simulation of a stochastic model for heterogeneous growth in the presence of a spatially varying temperature field and the comparison with a deterministic model obtained under the assumption that nucleation is much faster than growth, so that averaging is possible based on a multiple scale idea. Both models have been introduced and described in detail by the authors (cf. [2,16,17]); we will give a short exposition in section 2. The problem of simulation is discussed including various aspects in sections 3 and 4. In the latter we will put special emphasis on the problem of computing the mean density of interfaces of crystals ($\mu_{d,d-1}$, for $d = 1$ and $d = 2$). We will finally conclude and discuss some open

problems related with the numerical simulation and optimal control of nonisothermal crystallization in section 6.

2. Mathematical modelling

In the following we will review the development of mathematical models for nonisothermal crystallization in a stochastic as well as in a deterministic setup. The stochasticity of the crystallization process is caused by the randomness of the nucleation events, the standard model for nucleation is an heterogeneous Poisson-like process in space and time (with rate $\alpha = \alpha(x,t)$, cf., e.g., [2,16]). In an experimental situation, where heterogeneities are caused only by the heat transfer in the material, the nucleation rate can be modelled as a temperature-dependent material function (cf. [2,3]) of the form

$$\alpha(x,t) = \frac{\partial}{\partial t}\widetilde{N}\big(T(x,t)\big) + \dot{N}\big(T(x,t)\big). \tag{2.1}$$

This assumption is due to experimental observations which show that nucleation events are mainly caused by cooling (*athermal nucleation*), but in many materials still some rare nucleations may be observed when the cooling is stopped (i.e., when $\partial T/\partial t = 0$) at a temperature between the melting and the glass transition point. Since the term $\dot{N}$ responsible of nucleation without cooling (*thermal nucleation*) is much smaller than the term $\widetilde{N}$ in general, we restrict our attention to the case $\dot{N} = 0$ in the following, but we note that all models and methods may be adapted easily to the more general case (2.1).

Crystal growth can be modelled as a deterministic process; the evolution of the indicator function f^j of the crystal Θ_j is determined by the nonlinear initial-value problem

$$\frac{\partial f^j}{\partial t} + G\big|\nabla f^j\big| = 0 \quad \text{in } E \times (T_j, \infty), \tag{2.2}$$

$$\frac{\partial f^j}{\partial t} = \delta(\cdot - X_j) \qquad \text{in } E \times \{T_j\}, \tag{2.3}$$

where X_j and T_j are location and time of the birth of the crystal (cf. [16,18]) and G denotes the normal speed of growth (the *growth rate*). An experimentally verified model for the growth rate is pure temperature-dependence, i.e.,

$$G(x,t) = \widetilde{G}\big(T(x,t)\big). \tag{2.4}$$

The experimental results for $\widetilde{G}$ in the case of isotactic polypropylene are shown in figure 5. The indicator function $f = I_{\Theta^t}$ is determined by the indicator functions f^j via

$$f(x,t) = 1 - \prod_{T_j \leqslant t} \big(1 - f^j(x,t)\big). \tag{2.5}$$

The above considerations allow us to compute a realization of the stochastic crystallization process if the temperature field is known. The temperature T is determined by the standard heat equation together with a source arising from the latent heat, which is released at the moment of phase change and causes an immediate rise of temperature, more precisely,

$$(\rho c T)_t = \nabla \cdot (\kappa \nabla T) + (h I_{\Theta^t})_t \quad \text{in } E \times \mathbb{R}^+, \tag{2.6}$$

$$T = T^1 \quad \text{on } \partial E \times \mathbb{R}^+, \tag{2.7}$$

$$T = T^0 \quad \text{in } E \times \{0\}, \tag{2.8}$$

where equation (2.6) has to be understood in a weak sense. Here ρ denotes the density, c the heat capacity, κ the heat conductivity, and h the latent heat.

This heat transfer model is a random differential equation, since all parameters depend upon the random variable I_{Θ^t}. A direct consequence is the stochasticity of the temperature, whose evolution depends upon the change of the crystalline phase. The complete stochastic model of the crystallization process is given by the random differential equations (2.2)–(2.8) together with the Poisson process $\{(X_j, T_j)\}$.

In many industrial applications cooling is large, which implies together with the scale of $\widetilde{N}$ (varying from around 10^6 m^{-1} in $\mathbb{R}^1$ up to around 10^{16} m^{-3} in $\mathbb{R}^3$) that the number of nuclei per unit volume is very large. On the contrary, the growth rate is quite small (below 10^{-5} m$\cdot$s^{-1}), and consequently, we may expect many and small crystals. The typical scale of the heat transfer problem is given by

$$x_T = \sqrt{\frac{\kappa_0 t_0}{\rho_0 c_0}}, \tag{2.9}$$

where t_0 is the length of the considered time interval, κ_0, ρ_0 and c_0 are typical scales for κ, ρ and c. The typical scale for the growth of a nucleus is given by

$$x_G = G_0 t_0, \tag{2.10}$$

where G_0 is a typical value for the growth rate G. In practical applications it turns out that $x_T \gg x_G$, which is due to the fact that crystal growth is very slow, compared with heat conduction. This means that there exist two significant scales for the system, i.e.,

- a microscale (of size x_G) for growth,
- a macroscale (of size x_T) for heat conduction.

The scale of real interest in polymer processing is a *mesoscale* between x_T and x_G, which is sufficiently small with respect to the macroscale so that temperature may be considered approximately constant at that scale, but large enough with respect to the microscale so that it contains a large number of crystals. On such a mesoscale the description by an averaged deterministic model (cf. [2,16,17]) is possible, describing the evolution of ξ, u, v and T, which represent averaged quantities for the crystallinity

function, the free surface densities of crystals and temperature. The resulting system consists of deterministic partial differential equations given by

$$\frac{\partial \xi}{\partial t} = \widetilde{G}(T)(1-\xi)u, \tag{2.11}$$

$$\frac{\partial u}{\partial t} = \nabla \cdot \big(\widetilde{G}(T)v\big) + \mathcal{F}_d\big[\widetilde{G}, \widetilde{N}, T\big], \tag{2.12}$$

$$\frac{\partial v}{\partial t} = \nabla\big(\widetilde{G}(T)u\big), \tag{2.13}$$

$$\frac{\partial T}{\partial t} = \frac{1}{\rho c}\nabla \cdot (k\nabla T) + \frac{h}{c}\frac{\partial \xi}{\partial t}, \tag{2.14}$$

in $E \times (0, t_*)$, supplemented by the boundary conditions

$$u + v^T n = 0, \tag{2.15}$$

$$\frac{\partial T}{\partial n} = \alpha\big(T - T^1\big), \tag{2.16}$$

on $\partial E \times (0, t_*)$, and initial values given by

$$\xi = 0, \tag{2.17}$$

$$u = 0, \tag{2.18}$$

$$v = 0, \tag{2.19}$$

$$T = T^0, \tag{2.20}$$

in $E \times \{0\}$, usually with $T^0(x) \geqslant T_{\mathrm{m}}$ (melting temperature) for all $x \in E$. The source term $\mathcal{F}_d$ is a nonlinear operator dependent upon the spatial dimension; it is just the expected value of the rate of surface production by the crystals, more precisely (if $\widetilde{N}(T^0) = 0$, cf. [16,17])

$$\mathcal{F}_1\big[\widetilde{G}, \widetilde{N}, T\big](x,t) := 2\frac{\partial}{\partial t}\widetilde{N}\big(T(x,t)\big), \tag{2.21}$$

$$\mathcal{F}_2\big[\widetilde{G}, \widetilde{N}, T\big](x,t) := 2\pi\widetilde{G}\big(T(x,t)\big)\widetilde{N}\big(T(x,t)\big), \tag{2.22}$$

$$\mathcal{F}_3\big[\widetilde{G}, \widetilde{N}, T\big](x,t) := 8\pi\widetilde{G}\big(T(x,t)\big)\int_0^t \widetilde{G}\big(T(x,s)\big)\widetilde{N}\big(T(x,s)\big)\,\mathrm{d}s. \tag{2.23}$$

3. Numerical methods for the averaged model

An algorithm for the numerical approximation of the averaged model (2.11)–(2.20) has been proposed in [17] and analyzed with respect to convergence (cf. [19]). The basic idea of this algorithm is to perform an explicit time step in the hyperbolic part of the system together with an implicit step in the heat equation, which yields a decoupling and partial linearization in each time step. In semidiscrete form, this strategy for the hyperbolic part reads

$$\xi^{j+1} = \xi^j + \tau^j\big(1-\xi^j\big)\widetilde{G}\big(T^j\big)u^j, \tag{3.1}$$

$$u^{j+1} = v^j + \tau^j\big(\nabla\big(\widetilde{G}\big(T^j\big)v^j\big) + \mathcal{F}_d\big[\widetilde{G}, Nt, T^j\big]\big), \tag{3.2}$$

$$v^{j+1} = w^j + \tau^j\big(\nabla\big(\widetilde{G}\big(T^j\big)u^j\big)\big). \tag{3.3}$$

By the index j we denote the function at time t^j, and $\tau^j = t^{j+1} - t^j$ is the jth time step. For the full discretization any appropriate method like Lax's method (cf. [20]) or the Lax–Wendroff method for problems with source terms (cf. [20–22]) can be used. The stability bound for these methods is given by the Courant–Friedrichs–Levy condition (cf. [20,23]), i.e.,

$$2(\max G)\tau \leqslant \Delta x. \tag{3.4}$$

Because of the small size of G, this bound is not very restrictive and still allows a good performance of the algorithm.

For the numerical approximation of the parabolic part one can then use standard discretization methods like the Crank–Nicholson scheme, since the source including ξ is known at time $t = t^{j+1}$. Hence, we can solve the model equations efficiently by the following algorithm:

Algorithm 3.1 (Numerical solution of the averaged model).
Set the initial values $\xi^0 = u^0 = v^0 = 0$.
for $j = 0$ **to** $n-1$ **do**

1. Compute $\mathcal{F}_d[\widetilde{G}, \widetilde{N}, T^j]$.
2. Compute u^{j+1} and v^{j+1} by an explicit step for (2.12), (2.13), (2.15).
3. Compute ξ^{j+1} by an implicit (with respect to u) or explicit step in (2.11).
4. Solve the heat equation (2.14), (2.16) in $[t_j, t_{j+1})$ using ξ^{j+1} and ξ^j for the right-hand side to obtain T^{j+1}.

end

4. Simulation of the stochastic model

We turn our attention to an (efficient) simulation of the stochastic model (i.e., (2.6)–(2.7), coupled with the stochastic evolution of the term I_{Θ^t}), which consists of three main parts:

- *Nucleation*, which is the part with intrinsic stochasticity.
- *Growth* of the crystals nucleated at random locations.
- *Heat conduction*, which is influenced by the crystalline phase.

We put a special emphasis on the computation of the boundary densities of the crystals $\mu_{d,d-1}$, which will be denoted shortly by S_V below (the symbol S_V in place of $\mu_{d,d-1}$ is commonly used by some authors [24] to denote the (mean) surface density per

unit volume of a random set). The boundary density corresponds to the mean number of vertices of crystals per unit length, when $d = 1$, and to the mean length of boundary segments of crystals per unit area, when $d = 2$.

4.1. Nucleation

Since the nucleation rate $\alpha(x, t)$ depends on space and time, the birth of new crystals may be represented by an inhomogeneous space-time Poisson process (see, e.g., [25,26]) having stochastic intensity α (actually $\alpha(1 - I_{\Theta^t})$, since crystals already covered at the time of their birth are not of interest).

A standard algorithm for the simulation of such processes is the *thinning* or *random sampling* method (see [27, p. 77]). This method consists in simulating an homogeneous Poisson process with constant intensity $\widehat{\alpha}$, satisfying

$$\alpha(x, t) \leqslant \widehat{\alpha} \quad \forall x \in E,\ t \in \mathbb{R}_+.$$

In a subsequent thinning step a uniformly distributed random variable $R_i \in [0, 1]$ is evaluated for each generated point $\{(x_i, t_i)\}$, which is then retained if $R_i > \alpha(x_i, t_i)/\widehat{\alpha}$. For our problem it turns out this algorithm enforces a very high computational effort, since the number of generated points is much larger than the number of points that are finally kept. Therefore, we use a different approach, taking into account the spatial discretization of the domain E. Suppose we have a decomposition

$$E = \bigcup_{i=1}^{m} E_i, \tag{4.1}$$

$$0 = t_0 < t_1 < \cdots < t_n = t_{\text{final}}, \tag{4.2}$$

with $\operatorname{diam} E_i$ and $|t_j - t_{j-1}|$ sufficiently small such that the intensity of the process can be well approximated by a constant in each space-time cylinder $E_i \times (t_j, t_{j-1})$. Then we can simulate the births in the time interval (t_j, t_{j+1}) via the following algorithm:

Algorithm 4.1 (Generation of births in the time interval (t_j, t_{j+1})).
for $i = 1$ **to** m **do**

1. Compute $\alpha_{ij} := \int_{t_j}^{t_{j+1}} \int_{E_i} \alpha(x, t)\, \mathrm{d}x\, \mathrm{d}t$.
2. Generate a random number P_i, Poisson distributed with intensity α_{ij}. This number represents the number of "virtual" births in the ith space cell of the discretization.
3. Generate P_i independent random numbers $U_1, \ldots, U_{P_i}$ having uniform distribution in the cell E_i. These numbers represent the locations of the new "virtual" nuclei in the cell E_i.
4. Check if the new "virtual" nuclei are already covered by the crystalline phase: if yes, delete them, otherwise add them to the set of nuclei.

end

Note that if we are not interested in the evolution of the interfaces between two crystals, but only in the evolution of the crystallinity, we may disregard the effects of impingement and do not need to perform step 4 in the previous algorithm. Indeed, a new "virtual" crystal that is inside another one will never grow out of it [25,26]. Hence, the indicator function I_{Θ^t} does not change because of the presence of the new "virtual" nuclei inside the crystalline phase.

4.2. Growth

Together with the nucleation, we have to simulate the growth of crystals and their interaction with heat transfer.

In spatial dimension one, a crystal Θ^k nucleated at (X_k, T_k) is an interval $[c_k, d_k]$, the evolution of the boundary is determined by

$$\frac{\mathrm{d}}{\mathrm{d}t}c_k(t) = -G\big(c_k(t), t\big), \qquad \frac{\mathrm{d}}{\mathrm{d}t}d_k(t) = G\big(d_k(t), t\big), \tag{4.3}$$

with initial values $c_k(T_k) = d_k(T_k) = X_k$. Hence, an obvious way to compute the growth of a single crystal is to apply a numerical scheme to the nonlinear ordinary differential equations (4.3). Since the time steps and the increments in G are usually very small in realistic simulations, even an explicit method yields reasonable results. Hence, if impingement is disregarded and we are interested only in the evolution of I_{Θ^t}, growth can be computed according to the following algorithm:

Algorithm 4.2 (Growth of m one-dimensional crystals in the time interval (t_j, t_{j+1}) without impingement).
for $k = 1$ **to** m **do**

1. If $T_k \in (t_j, t_{j+1})$ set $c_k = d_k = X_k$ and $s = T_k$. Else, set $s = t_j$ if $T_k < t_j$ and $s = t_{j+1}$ if $T_k > t_{j+1}$.
2. Compute (or approximate) the growth rate at the boundary points of the kth crystal $[c_k, d_k]$:
$$G_1 = G\big(T(c_k, s)\big), \qquad G_2 = G\big(T(d_k, s)\big).$$
3. Update the boundary points by
$$c_k = c_k - G_1(t_{j+1} - s), \qquad d_k = d_k + G_2(t_{j+1} - s).$$

end

Of course, also more advanced schemes for the numerical integration of 4.3 can be used in algorithm 4.2, and the algorithm can in principle also be carried over to higher dimensions, where systems of ordinary differential equations can be derived for the evolution of each point on the boundary (cf. [16,19]), but then an additional discretization of the boundary of a crystal has to be performed (cf. [19]).

If we are interested also in the effects of impingement, i.e., in monitoring the evolution of the interface densities, Algorithm 4.2 has several disadvantages. Obviously, in one spatial dimension, one can check if two crystals Θ^j and Θ^k intersect by simply comparing c_k with d_j and d_k with c_j, but if we want to find all interfaces this method is computationally expensive. Therefore, it also seems necessary to derive a faster numerical method for the simulation of growth, which allows one to trace the interfaces efficiently also in higher spatial dimensions.

The clue for such a method seems to be a change from the Lagrangian perspective induced by (4.3) to an Eulerian approach, i.e., we fix locations in space and watch the crystals arriving. We use this Eulerian viewpoint for a "pixel colouring" technique, i.e., we assign a number (respectively a colour) to each crystal and then assign this number (colour) to the spatial locations (pixels) covered by the crystal. More precisely, we fix a spatial grid (usually finer than the grid on which the temperature is assigned, because of the larger scale of heat conduction with respect to growth) in the domain E and at every time step we check for each grid point if it is inside a crystal (which is the case if there exist a grid point of radial distance less than $G\Delta t$); if yes, we assign the number of the crystal to this point (respectively colour it). An additional speed-up can be achieved by marking those grid points, which are at the boundary of a crystal and computing the growth only there (all the points in the interior of a crystal do not provide additional information).

If we have K_j marked pixels at time t_j (i.e., the ones which are coloured and at the boundary of a crystal), then we simulate the growth in a time step (t_j, t_{j+1}) in the following way:

Algorithm 4.3 (Growth in a time interval (t_j, t_{j+1}) with impingement).
for $k = 1$ **to** K_j **do**

1. Compute the growth rate at the pixel p_k: $G_k = G(T(p_k, t_j))$.
2. Compute the radius associated with the pixel p_k: $\Delta r_k = G_k(t_{j+1} - t_j)$.
3. **For** every pixel p included in a disk centered at p_k having radius Δr_k **do**
   - If p is not in the crystalline phase (uncoloured), assign to p the same number of p_k (colouring), mark p and compute the approximate time at which it is captured by p_k: $\tau_k = \|p - p_k\|/G_k$.
   - If p is already inside a crystal (i.e., it has been captured at a time τ) and is marked, compute the time at which it is captured by p_k: $\tau_k = \|p - p_k\|/G_k$. If $\tau_k < \tau$, assign to p the number (colour) of p_k .

   end
4. Unmark pixel p_k.

end

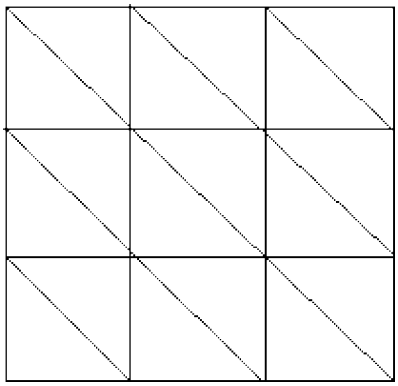

Figure 3. Triangular mesh used for the finite element discretization of equation (4.4).

We note that step 3 ensures that every pixel assumes the colour of the first crystal by which it is reached, independently from the order of checking of the marked pixels and of the chosen time step. The accuracy of the algorithm increases as the step size in time and the spatial grid size decrease; obviously they cannot be chosen independently, since one should ensure that a crystal can really reach neighbouring grid points in one time step, i.e., if h is the typical grid size and Δt the time step we need at least $h < G_0 \Delta t$, where G_0 is a typical value of the growth rate.

4.3. An algorithm for the complete model

For the temperature we have to solve an equation of the form

$$T_t = \operatorname{div}(D \nabla T) + L \frac{\partial}{\partial t} I_{\Theta^t}. \tag{4.4}$$

The discretization can be performed via finite elements; we have used linear finite elements on a triangular mesh of the type shown in figure 3. The numerical method used for the discretization of the stochastic term must be explicit, since the birth-and-growth process is unpredictable. Because of the larger scale of heat conduction, we propose to use a coarser grid for the heat equation than for the computation of growth. The use of linear finite elements leads to a finite differences discretization for the diffusion term and to a "smoothening" (spatial integral) of the source term via the test functions. With the above approximations we can simulate the complete process as follows:

Algorithm 4.4 (Stochastic simulation of nonisothermal crystallization).
Start with the initial temperature T^0 and set $\Theta^0 = \emptyset$.
Set $j = 0$: solve the discretized version of equation (4.4) via linear finite elements and $f^0(x) = f^1(x) = 0 \; \forall x \in E$ to obtain T^1.
for $j = 1$ to $n - 1$ **do**

1. Approximate the nucleation rate in $[t_j, t_{j+1})$ by
$$\alpha \sim \frac{\mathrm{d}\widetilde{N}}{\mathrm{d}T}\frac{T^j - T^{j-1}}{t_j - t_{j-1}}.$$
2. Simulate the nucleation in $E \times [t_j, t_{j+1})$ according to algorithm 4.1 and add the new generated nuclei to $\Theta^{t_{j+1}}$.
3. Let the (old and new) crystals grow until time t_{j+1} and update $\Theta^{t_{j+1}}$.
4. Compute the indicator function $f^{j+1}(x) = I_{\Theta^{t_{j+1}}}(x)$.
5. Solve the discretized heat equation to obtain T^{j+1}.

end

4.4. Computation of the surface density

In the one-dimensional case, the surface density can be computed easily from the result of Algorithm 4.3 by counting the number of times that there is a colour change in the pixels, moving in the interval E from its left to the right boundary point.

In two (or three) spatial dimensions, Algorithm 4.3 provides at every time step a 2D (or 3D) matrix, in which different integer numbers (representing the colours) correspond to different crystals, usually the empty space corresponds to the number 0. This vector may be easily used to compute the mean local surface density of crystals $S_V(x)$ (i.e., the mean length of edges of crystals per unit area). The method that we propose is based on the estimate of the *spherical contact distribution function* [24,28].

Definition 4.5. Let Θ be a random closed set. Then the associated local spherical contact distribution function is
$$H_s(r, x) := P\big(x \in \Theta \oplus b(0, r) \mid x \notin \Theta\big),$$
where $\oplus$ denotes Minkowski addition and $b(0, r)$ is a d-dimensional ball of radius r, centered at the origin.

The estimate of S_V is possible thanks to the following theorem, which has been proven in [28].

Theorem 4.6. Let $\Xi(t) = \bigcup_i \partial C_i(t)$ be the (random) set of the boundaries of the cells of an (incomplete) Johnson–Mehl tessellation at time t, having Hausdorff dimension $d - 1$. Let $H_s(r, x, t)$ be the local spherical contact distribution function associated with $\Xi(t)$ and let $\Xi_r(t)$ be the parallel set of radius r of $\Xi(t)$
$$\Xi_r(t) = \Xi(t) \oplus b(0, r),$$
where $b(x, r)$ is a d-dimensional ball of radius r centered at X. If the condition
$$\lim_{r\to 0} \frac{\nu_d[\Xi_r(t) \cap b(x, \varepsilon)]}{r} = 2\nu_{d-1}\big(\partial\Xi(t) \cap b(x, \varepsilon)\big) \tag{4.5}$$

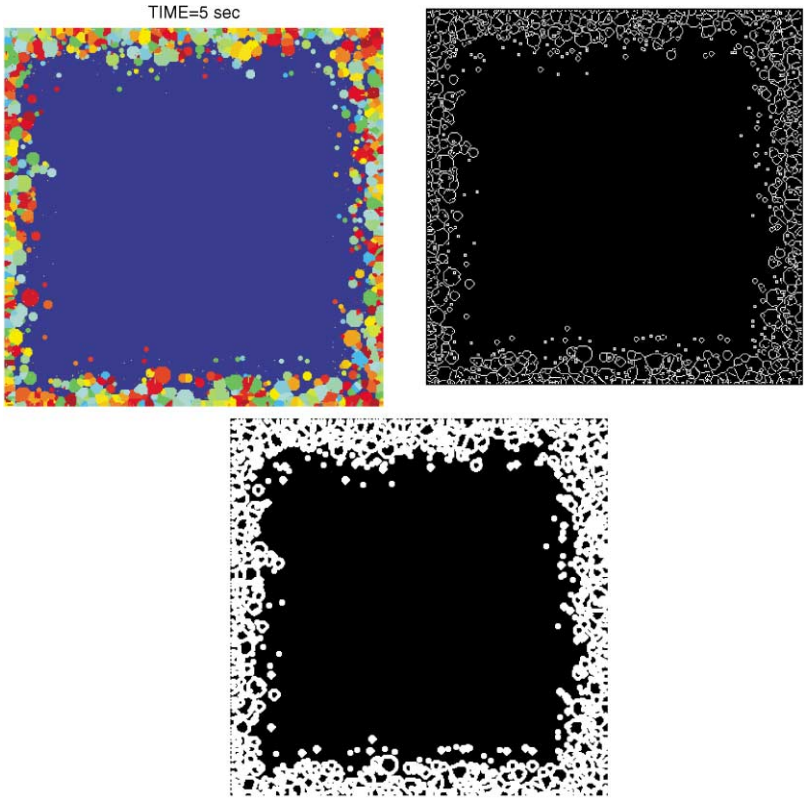

Figure 4. Top left: a simulated crystallization process. Top right: boundaries are recovered via an image analiser. Bottom: parallel set of radius r of the detected boundaries.

is satisfied for all $x \in \mathbb{R}^d$ and for all $\varepsilon \in \mathbb{R}_+$, then the function $H_s(r, x, t)$ is differentiable at $r = 0$ for ν_d-almost all x, and its derivative satisfies

$$\frac{\mathrm{d}}{\mathrm{d}r} H_s(r, x, t)|_{r=0} = 2S_V(x, t). \tag{4.6}$$

Formula (4.6) may be used to estimate S_V from an estimator of H_s. Suppose to recover a black-and-white image of the boundaries of the simulated crystals, as shown in figure 4. Note that $H_s(r, x, t)$ equals the local volume density of the parallel set $\Xi_r(t)$ of $\Xi(t)$ (since $P(x \notin \Xi(t)) = 1$ so that $H_s(r, x, t) = P(x \in \Xi(t) + b(0, r)) = P(x \in \Xi_r(t))$), which is in general nonzero, being $\Xi_r(t)$ a set of Hausdorff dimension d.

The (local) volume density $\xi(x)$ of a random set Θ can be estimated by considering an observation window $W(x)$, centered at x, sufficiently small so that the volume density may be considered constant inside the window, but not too small with respect to the size of the random set (if possible), so that the probability that the window is completely occupied by the set or completely empty is nontrivial, i.e., is not 0 or 1 (usually if the random set Θ is a 2D black and white digitized image, the window $W(x)$ must be chosen

much larger than the size of a pixel). Then a grid $x_1, \ldots, x_n$ of n points is overlapped to the window $W(x)$ and the local volume density of Θ is estimated by

$$\widehat{\xi}(x) = \frac{1}{n} \sum_{i=1}^{n} \mathbf{I}_{\Theta}(x_i).$$

This estimator is unbiased, with variance

$$\sigma^2 = \frac{1}{n^2} \Big(n\xi(x)\big(1 - \xi(x)\big) + 2 \sum_{i>j} k(r_{ij}) \Big),$$

where $r_{ij} = \|x_i - x_j\|$ and k is the covariance function of Θ (see [24] for further details). Thus, in our case an unbiased estimator of $H_s(r, x, t)$ in a window $W(x)$, with a grid $x_1, \ldots, x_n$, is

$$\widehat{H}_s(r, x, t) = \frac{1}{n} \sum_{i=1}^{n} \mathbf{I}_{\Xi_r(t)}(x_i).$$

An estimator of $(\mathrm{d}/\mathrm{d}r) H_s(r, x, t)|_{r=0}$ may be obtained by numerical approximation

$$\frac{\partial}{\partial r} \widehat{H}_s(r, x, t)|_{r=0} \approx \frac{4\widehat{H}_s(r, x, t) - \widehat{H}_S(2r, x, t)}{2r},$$

for $r > 0$ small, since $H_s(0, x, t) = 0 \; \forall x \in \mathbb{R}^d, \forall t \in \mathbb{R}_+$ (this is a second-order scheme, so that the resulting error is $\mathrm{o}(r^2)$). Thus, an estimator of the surface density $S_V(x, t)$ of the random tessellation is

$$\widehat{S}_V(x, t) = \frac{1}{2} \frac{\widehat{H}_s(r, x, t)}{r} = \frac{1}{2nr} \sum_{i=1}^{n} \mathbf{I}_{\Xi_r(t)}(x_i).$$

5. Numerical results

For numerical experiments we used data from isotactic polypropylene (i-PP). Referring to the notations of equation (2.6), the quantities h, ρ, c, k have been assumed to be constant and equal in the amorphous and in the crystalline phase, since their variability for i-PP is relatively small. Thus, equations (2.6) and (2.7) may be rewritten as

$$T_t = D\Delta T + L(I_{\Theta^t})_t \quad \text{in } E \times \mathbb{R}^+, \tag{5.1}$$

$$T = T_{\text{out}} \quad \text{on } \partial E \times \mathbb{R}^+, \tag{5.2}$$

with $D = 0.5 \text{ m}^2/\text{s}$ and $L = 50°\text{C}$, which correspond to mean values of experimental data.

For the nucleation and growth rate we used curves fitted to experimental data from [26] of the form

$$\widetilde{G}(T) = 10^{y(T)}, \qquad \widetilde{N}(T) = 10^{z(T)},$$

where y is a piecewise quadratic and z is a piecewise linear spline (see figure 5).

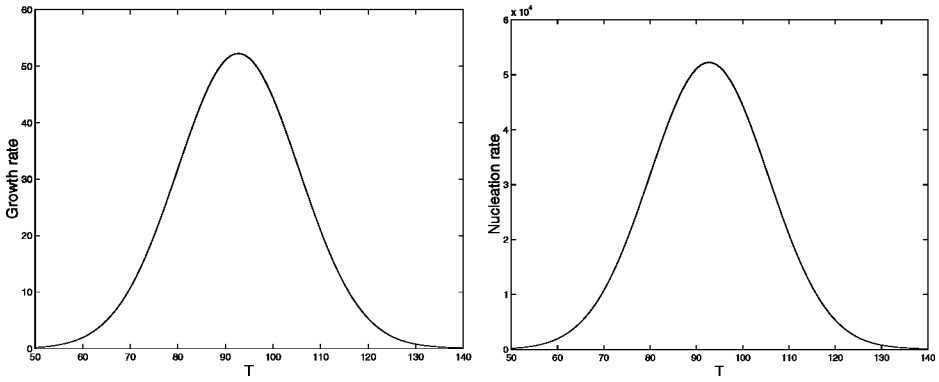

Figure 5. Growth rate $\widetilde{G}(T)$ (left) and nucleation rate $\widetilde{N}(T)$ (right) as functions of temperature T.

All algorithms have been implemented with the Scientific Computing Tool MATLAB, which was also used for the image analysis and visualization of results.

5.1. Numerical results in $\mathbb{R}^1$

The results of a one-dimensional stochastic simulation are shown in figure 6. The simulation has been performed starting from a uniform temperature of 130°C in the whole domain $E = (0, 1)$ at time $t = 0$ and suddenly cooling the boundary points to 80°C. The result clearly shows the strong effects on temperature due to the release of latent heat and due to the small diffusion coefficient. The peaks in the temperature profile are caused by new nucleations; they are smoothed in time because of diffusion. If the temperature is kept only slightly below the melting point, the increase of temperature due to the phase change may even stop the growth of nucleated crystals. This is evident if we take into account impingement in the simulation, obtaining, thus, results as shown in figures 7 and 8. In figure 8 the cones of influence of crystals are plotted, i.e., the space–time region occupied by each growing crystal. It can be seen that already before two crystals hit each other, their growth is almost stopped for a certain time because of the increase of temperature and the consequent decrease of the growth rate.

A comparison of the results obtained from the stochastic model (2.6) and from the deterministic system (2.11)–(2.14) is shown in figure 9. To compare the two models, 100 stochastic simulations, independent but with the same parameters, have been performed. The crystallinity at time t has then been computed by averaging, both in space and time, of the indicator function I_{Θ^t} computed in each stochastic simulation. The result is compared with the correspondent crystallinity obtained by the deterministic model (left); the same averaging procedure is applied to the temperature field, too. The plot of the deterministic (solid) and averaged stochastic quantities (dashed), shows good agreement in general, in particular for the degree of crystallinity. The results for temperature shows that the deterministic model seems to react more slowly to changes in the source term.

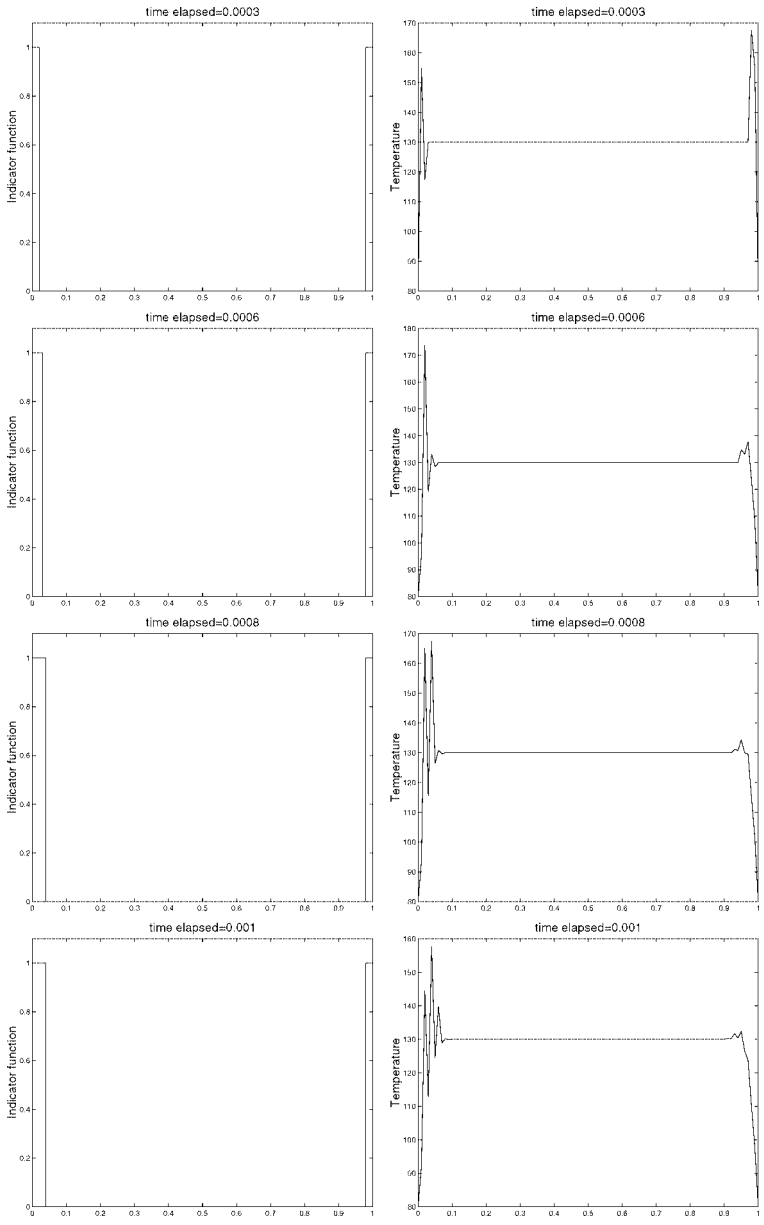

Figure 6. Evolution of the indicator I_{Θ^t} (left) and of the temperature field (right) in a 1D stochastic simulation with growth computed disregarding impingement.

Figure 7. Result of a 1D stochastic simulation with growth computed with the "pixel colouring" technique. The blue zones are empty.

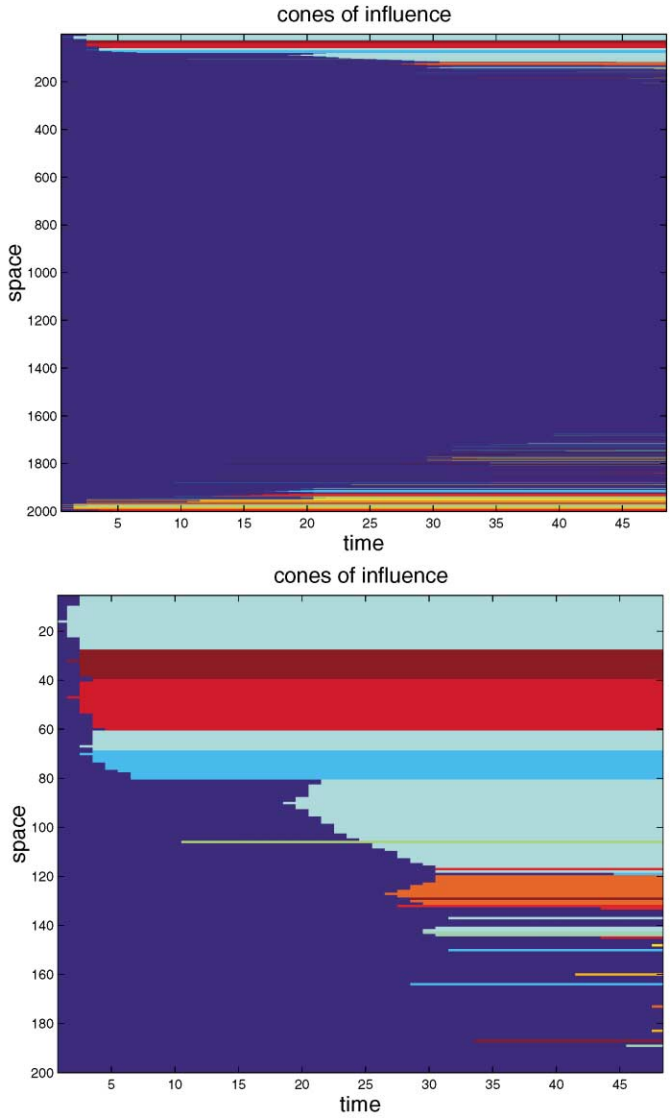

Figure 8. Cones of influence in a 1D stochastic simulation (top) and a zoom of the same image (bottom). Note that the growth of some crystals is stopped before impingement occurs by the increase of temperature due to the release of latent heat.

We imposed a ratio between the nucleation rate α and the growth rate $\widetilde{G}$ of the order of 10^3 (in many practical examples it is much larger). It can be seen from the pictures that already with this relatively small ratio between the two quantities the numerical results are quite similar. Due to averaging arguments based on the law of large numbers we expect an improvement for increasing nucleation rate, but so far we were not able to realize such a case in reasonable computational time.

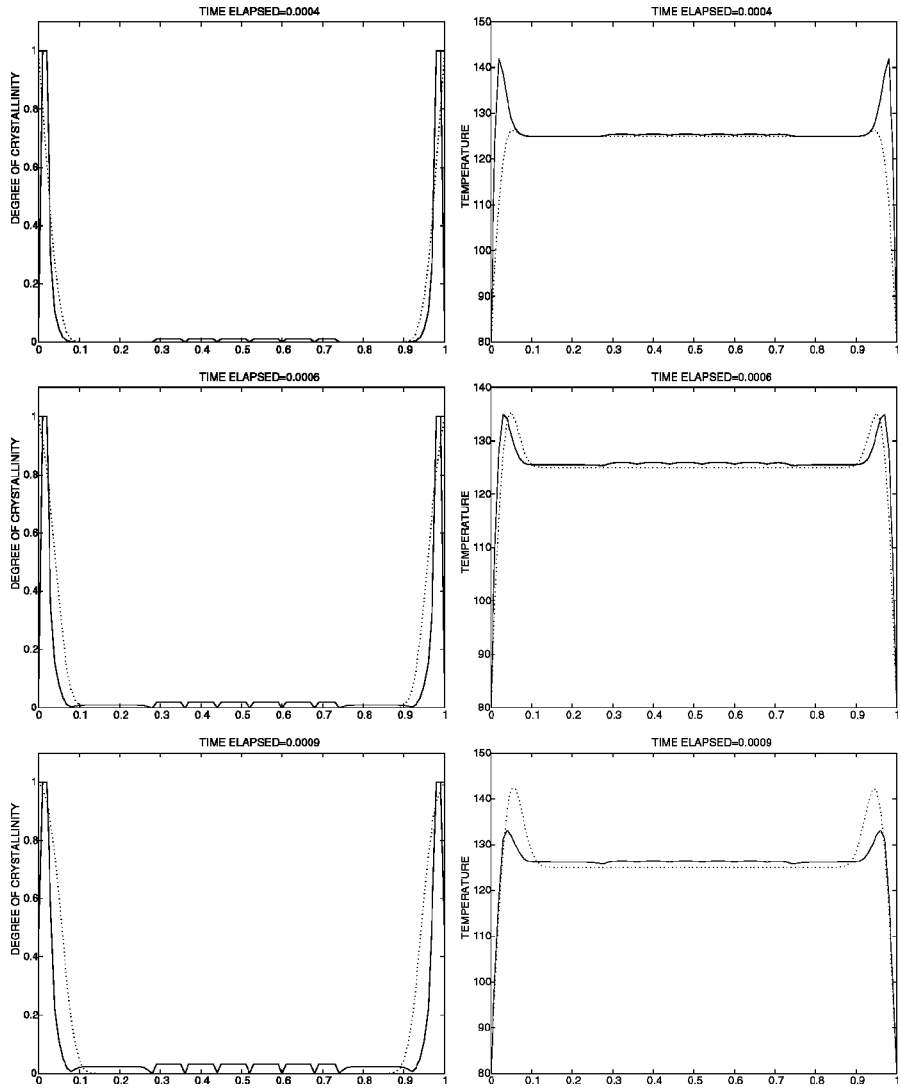

Figure 9. Evolution of the crystallinity (on the left) and of the mean temperature (on the right) in the stochastic and the deterministic models. The solid lines are the solutions of the deterministic model, the dashed lines are the means of the stochastic simulations.

5.2. Numerical results in $\mathbb{R}^2$

A two-dimensional numerical experiment was performed on a rectangle, with the same data for the parameters as in the one-dimensional case. We cooled the sample starting from a uniform temperature of 120°C and then cooling the boundary with constant speed $\partial T/\partial t|_{\partial E} = 0.5\ \mathrm{K{\cdot}s^{-1}}$. The results are shown in figures 10 and 11, the behaviour is similar to the one-dimensional example; most crystals nucleate close to the boundary, while the temperature in the interior is too high for significant nucleation.

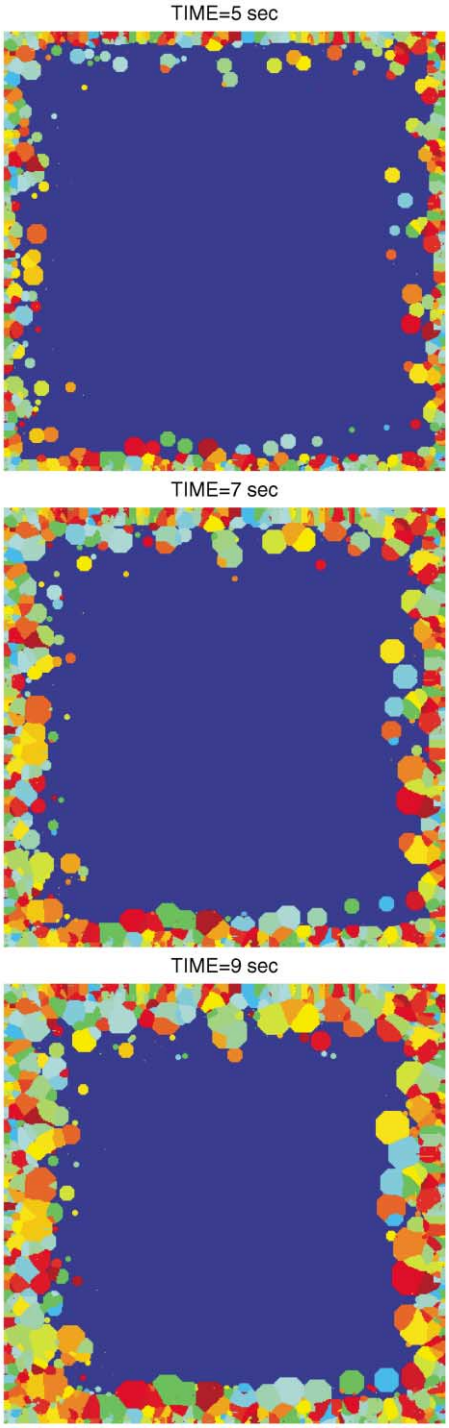

Figure 10. Evolution of the crystals in the stochastic simulation with cooling at the boundary.

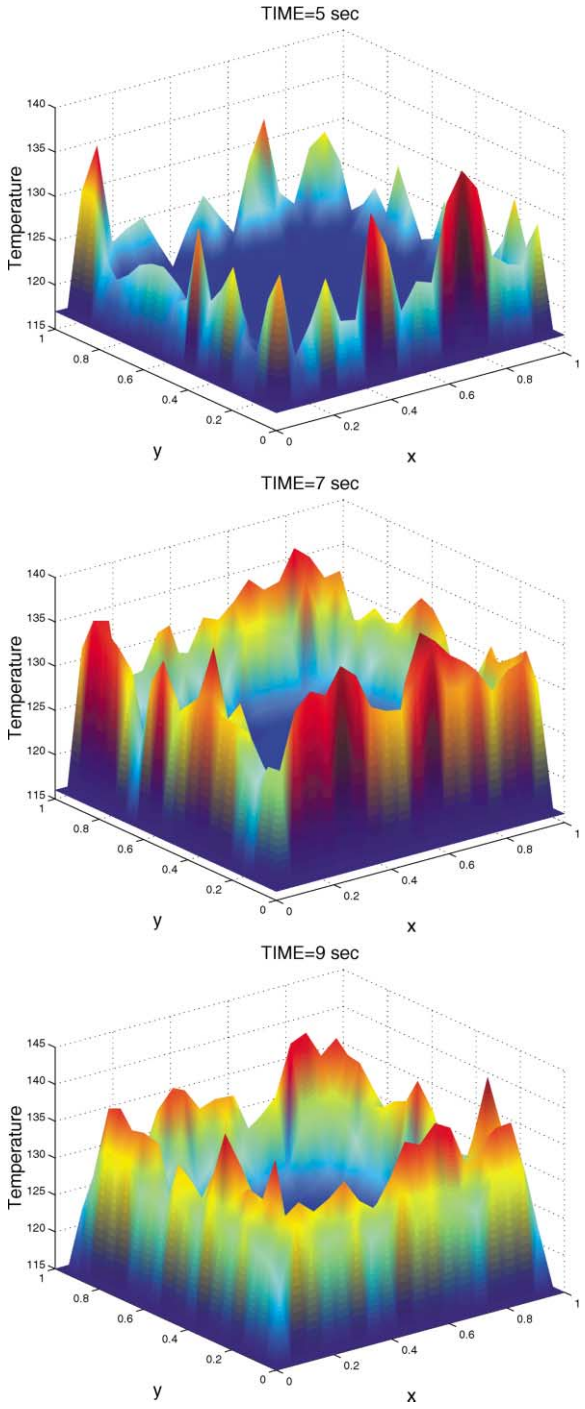

Figure 11. Evolution of the temperature field corresponding to the stochastic simulation of figure 10 with cooling at the boundary.

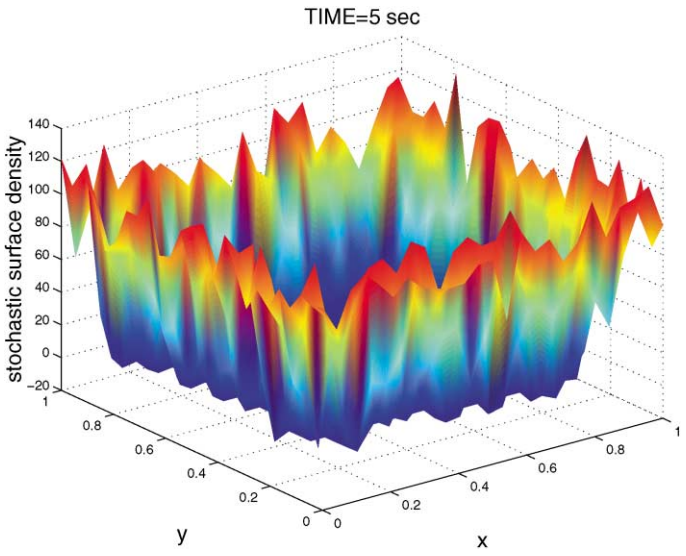

Figure 12. Surface density computed at time $t = 5$ s on a single simulation.

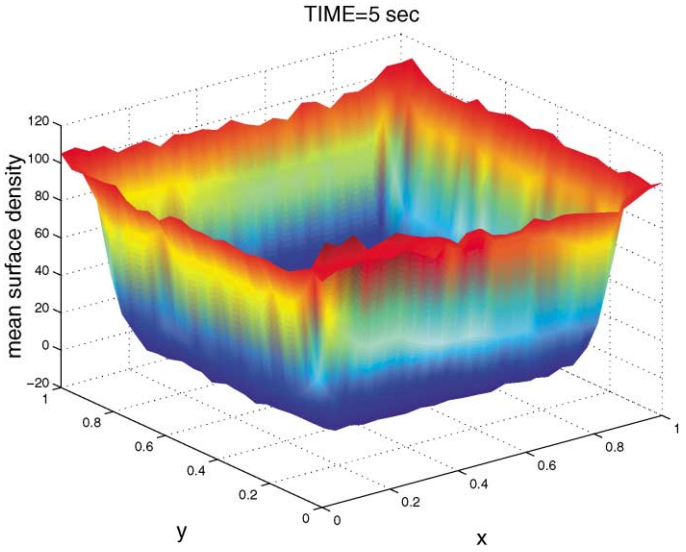

Figure 13. Estimated mean surface density $\overline{S}_V(x)$, computed at time $t = 5$ s averaging the stochastic content of interfaces over 50 simulations.

The generated morphology is typical for an experiment with boundary cooling, where there are many fine grains close to the boundary and few larger ones inside. In figure 12 the estimated stochastic surface density $\widehat{S}_V$, computed at time 5 s, is plotted. Its mean $\overline{S}_V(x)$ computed on 50 simulations is plotted in figure 13.

6. Conclusions and open problems

We have shown above how nonisothermal crystallization can be simulated either by a stochastic or a deterministic approach. While the deterministic model is based on an approximation that works only under certain conditions (many and small crystals), the stochastic simulation is expected to yield reasonable results in any case. Although the numerical effort could be reduced significantly by algorithm 4.3 with respect to the first approach, it is still very expensive to perform numerical experiments, in particular in $\mathbb{R}^3$. The improvement of the methods used for computing as well as a rigorous mathematical analysis are open problems for future work.

We note that real chemical experiments of the same kind could be performed in a lab, by using thin slices of polymeric material, and cooling them via a thermostat to control the temperature in the whole slice. The disadvantage of this technique is that interfaces are often not clearly visible from microscope images of the crystallized material, in particular when the number of generated crystals is very large. Instead it is rather simple to distinguish and measure the length of the interfaces generated by the simulator, by using some edge detector or image analizer. In practical applications, the approximation by the simulator are much smaller than the information that can be extracted from a picture of a real crystallized sample. Hence, this is a typical example in which simulated data may effectively substitute the experimental ones.

Another problem related to the simulation of nonisothermal crystallization is the optimal control of the process. In order to obtain good mechanical properties of the solidified material, a uniform grain size distribution is desired. As we have seen in our numerical experiments, a simple cooling strategy will not yield this result. Therefore, one wants to find a temperature $T^1 = T^1(x, t)$ in the boundary condition

$$\frac{\partial T}{\partial n} = \alpha\big(T - T^1\big) \tag{6.1}$$

such that the densities of the interfaces or the crystal sizes are as much uniform as possible.

Acknowledgements

Fruitful and stimulating discussions are acknowledged to Prof. Vincenzo Capasso (MIRIAM, University of Milano, Italy), Dr. Claudia Salani (MIRIAM, University of Milano, Italy), Prof. G.C. Alfonso (Department of Chemistry and Industrial Chemistry, University of Genova, Italy), Prof. G. Eder (Department of Chemistry, University of Linz, Austria), Dr. Stefano Micheletti (Department of Mathematics, Politecnico di Milano), Prof. C. Verdi (Department of Mathematics, University od Milan). Financial support is acknowledged to the Austrian Fonds zur Förderung der wissenschaftlichen Arbeit, Projects P 13478-INF and SFB F 013, to the EU under the TMR-Network *Differential Equations in Industry and Commerce*, to the Italian MURST/cofin. Pro-

gramme “Stochastic processes with spatial structure” and to the Italian CNR contract No. 98.03635.ST74.

References

[1] G. Matheron, *Random Sets and Integral Geometry* (Wiley, New York, 1975).
[2] M. Burger, V. Capasso and G. Eder, Modelling crystallization of polymers in temperature fields, Z. Angew. Math. Mech. (2001) (to appear).
[3] G. Eder, Mathematical modelling of crystallization processes as occurring in polymer processing, Nonlinear Anal. 30 (1997) 3807–3815.
[4] M. Avrami, Kinetics of phase change I–III, J. Chem. Phys. 7 (1939) 1103–1112; 8 (1940) 212–224; 9 (1941) 177–184.
[5] V.R. Evans, The laws of expanding circles and spheres in relation to the lateral growth rate of surface films and the grain-size of metals, Trans. Faraday Soc. 41 (1945) 365–374.
[6] A.N. Kolmogorov, On the statistical theory of the crystallization of metals, Bull. Acad. Sci. USSR Math. Ser. 1 (1937) 355–359.
[7] V. Capasso, M. De Giosa, A. Micheletti and R. Mininni, Stochastic modelling and statistics of polymer crystallization processes, Surveys Math. Indust. 6 (1996) 109–132.
[8] V. Capasso, I. Gialdini and A. Micheletti, Stochastic modelling and morphological features of polymer crystallization processes, in: *Proceedings of the Eighth European Conference on Mathematics in Industry*, ed. M. Brons (Teubner, Stuttgart, 1996).
[9] G. Eder, Crystallization kinetic equations incorporating surface and bulk nucleation, Z. Angew. Math. Mech. 76(S4) (1996) 489–492.
[10] A. Micheletti and V. Capasso, The stochastic geometry of polymer crystallization processes, Stochastic Anal. Appl. 15 (1997) 355–373.
[11] G. Eder and H. Janeschitz-Kriegl, Structure development during processing: Crystallization, in: *Materials Science and Technology*, Vol. 18, ed. H. Meijer (Verlag Chemie, Weinheim, 1997).
[12] V. Capasso, A. Micheletti and G. Eder, Polymer crystallization processes and incomplete Johnson–Mehl tessellations, in: *Progress in Industrial Mathematics at ECMI98*, eds. L. Arkeryd, J. Bergh, P. Brenner and R. Petterson (Teubner, Stuttgart/Leipzig, 1999) pp. 130–137.
[13] J. Møller, Random Johnson–Mehl tessellations, Adv. Appl. Prob. 24 (1992) 814–844.
[14] A. Micheletti, V. Capasso and G. Eder, The density of n-facets of an incomplete Johnson–Mehl tesselation, Preprint 15/97, Industrial Mathematics Institute, University of Linz (1997).
[15] V. Capasso and A. Micheletti, Local spherical contact distribution function and local mean densities for inhomogeneous random sets, Stochastics Stoch. Rep. 72 (2000) 51–67.
[16] M. Burger, V. Capasso and C. Salani, Modelling multi-dimensional crystallization of polymers in interaction with heat transfer, Nonlinear Anal. Ser. B: Real World Applications (2001) (to appear).
[17] M. Burger and V. Capasso, Mathematical modelling and simulation of nonisothermal polymer crystallization, Math. Models Methods Appl. Sci. 11 (2001) 1029–1054.
[18] J.A. Sethian, *Level Set Methods. Evolving Interfaces in Geometry, Fluid Mechanics, Computer Vision, and Materials Science* (Cambridge University Press, Cambridge, 1996).
[19] M. Burger, Direct and inverse problems in polymer crystallization processes, PhD thesis, University of Linz (2000).
[20] H. Niessner, Stability of Lax–Wendroff methods extended to deal with source terms, Z. Angew. Math. Mech. 77 (Suppl. 2) (1997) S637–S638.
[21] R. LeVeque, *Numerical Methods for Conservation Laws* (Birkhäuser, Basel/Boston/Berlin, 1990).
[22] Y. Zhang and B. Tabarrok, Modifications to the Lax–Wendroff scheme for hyperbolic systems with source terms, Int. J. Numer. Methods Engrg. 44 (1999) 27–40.
[23] D. Kröner, *Numerical Schemes for Conservation Laws* (Wiley-Teubner, Chichester/Stuttgart, 1997).

[24] D. Stoyan, W.S. Kendall and J. Mecke, *Stochastic Geometry and Its Applications*, 2nd ed. (Akademie-Verlag, Berlin, 1995).
[25] V. Capasso and C. Salani, Stochastic birth and growth processes modelling crystallization of polymers with spatially heterogeneous parameters, Nonlinear Anal. 1 (2000) 485–498.
[26] C. Salani, On the mathematics of polymer crystallization processes: Stochastic and deterministic models, PhD thesis, Universitá di Milano (1999).
[27] S.M. Ross, *Simulation*, 2nd ed. (Academic Press, San Diego, 1997).
[28] A. Micheletti, The surface density of a random Johnson–Mehl tessellation, Preprint N. 17/2001, Department of Mathematics, University of Milan (2001).
[29] M. Burger, V. Capasso and H.W. Engl, Inverse problems related to crystallization of polymers, Inverse Problems 15 (1999) 155–173.
[30] J. Serra, *Image Analysis and Mathematical Morphology* (Academic Press, London, 1984).